Bull. Mater. Sci., Vol. 29, No. 5, October 2006, pp. 513–521. © Indian Academy of Sciences.

Morphology, surface topography and optical studies on electron beam evaporated MgO thin films

A CHOWDHURY* and J KUMAR

Materials Science Programme, Indian Institute of Technology, Kanpur 208 016, India

MS received 16 November 2005; revised 24 August 2006

Abstract. Electron beam evaporated thin films of MgO powder synthesized by burning of magnesium ribbon in air and sol–gel technique are studied for their microstructure (SEM), surface topography (AFM), and optical transmission behaviour (UV-visible spectroscopy). MgO thin films are shown to be either continuous or have mesh like morphology. The bar regions are believed to be of magnesium hydroxide formed due to absorption of moisture. Their AFM images exhibit columnar/pyramidal/truncated cone structure, providing support to the 3D Stranski–Krastanov model for film growth. Further, they are shown to have high transmittance (~90%) in the wavelength range 400–600 nm, but absorb radiation below 350 nm substantially giving signature of a band transition.

Keywords. Thin film; surface morphology; magnesium oxide.

1. Introduction

Magnesium oxide (MgO) thin films find several applications in the different developing areas of materials science and engineering. Its thin films find application as protective layer (Boeuf 2003) for plasma display panels (PDPs), an alternative dielectric to silicon dioxide (SiO_2), and dynode in electron multipliers in Zeus display panel, reflecting and antireflecting coatings (Chowdhury 2005). MgO/TiO_x superlattices (Imai *et al* 1992) have been synthesized on an MgO substrate for the combination of various thicknesses of titanium oxide layers and MgO layers. MgO single crystal is an excellent substrate for preparing ferroelectric and superconductor thin films (Phillipsa Julia 1996).

There are several methods by which MgO thin films have been prepared in the past. One popular choice is to use the pulsed laser deposition technique for MgO layers on GaAs (Nashimoto *et al* 1992). They found the best crystallographic quality at 350°C in 5×10^{-6} Torr O_2. Polycrystalline MgO films (Boo *et al* 1996) have been prepared on GaAs (100) substrates by low-pressure metal–organic chemical vapour deposition using Mg (2,2,6,6-tetramethyl-3,5-heptanedionate)$_2$ as a precursor and oxygen as a carrier gas. The major orientation has been found out to be in the [100] direction at the substrate temperature of 300°C. MgO thin films have been deposited on Si(111) substrates by atomic layer growth (ALG) using a hydrolysis surface reaction of $Mg(C_2H_5)_2$ and H_2O (Huang and Kitai Adrian 1992). Park *et al* (2000) studied surface-discharge characteristics of MgO thin films prepared by reactive RF unbalanced magnetron sputtering. Sol–gel synthesis of crystalline magnesium oxide (Chakrabarti *et al* 2002, 2003) has been reported on soda lime glass using non-alkoxide precursor chemicals for the first time. But they could not avoid the formation of magnesium hydroxide in their final films along with the presence of periclase and *b*-MgO phase. Ho *et al* (1997) prepared MgO thin films with either (111) or (200) preferential orientation on (100) Si substrates by sol–gel method followed by heat treatment at 800°C. But in almost all the application fields there is a common problem associated with it, i.e. the problem of hydration. Studies in the past (Kim *et al* 1994) suggest that during synthesis of MgO thin films aqueous/chemical (e.g. spin coating) route should be avoided. But still evidence of hydration has been noted also, which in turn deteriorates other properties, viz. optical, electronic etc. Here we report synthesis of magnesium oxide thin films by e-beam evaporation method with two different powders, viz. MgO powder obtained by burning of magnesium ribbon in air and powder obtained through sol–gel technique. Thin films have been subsequently prepared by electron beam evaporation method using the synthesized MgO powder and studied for their microstructure (SEM), surface topography (AFM), and optical transmission behaviour (UV-visible spectroscopy). Effect of annealing on the properties of thin films has also been investigated.

2. Experimental

Mostly, MgO thin films are extensively applied as protective layer for plasma display panels (PDPs) where thin MgO

*Author for correspondence (preac@leeds.ac.uk)

Table 1. List of raw materials used for the synthesis of MgO.

Materials	Specification
Magnesium acetate tetrahydrate $[(CH_3COO)_2Mg{\cdot}4H_2O]$	Chloride, 0·005%; sulphate, 0·01%; lead, 0·002%
Magnesium ribbon (Mg)	Lead, 0·01%; copper, 0·005%; iron, 0·05%; substances insoluble in HCl, 0·05%
Ethyl alcohol (C_2H_5OH)	Water, 0·1% v/v; acidity, 0·01 mln%; non-volatile matter, 0·001%; aldehydes and ketones, 0·005%; furfuraldehyde, 0·001%
Oxalic acid $[(COOH)_2{\cdot}2H_2O]$	Min. assay = 99·08%

Table 2. Sample code for MgO thin films.

Sl. no.	Pellet used as source material for electron beam evaporation	Annealing conditions	Sample code
1.	Pellet of MgO powders obtained by burning magnesium ribbon	Annealed at 500°C in presence of oxygen with a flow rate of 30 cc/s	A
2.		Annealed at 500°C in presence of air	B
3.		Nil	C
4.	MgO powders obtained by sol–gel method	Annealed at 500°C in presence of oxygen with a flow rate of 30 cc/s	D
5.		Annealed at 500°C in presence of air	E
6.		Nil	F

films are coated on glass substrates and hence glass substrates have been chosen for experimental purpose. The glass slides of size $25 \times 25 \times 1{\cdot}3$ mm were used as substrate. They were first cleaned with soap detergent as a routine cleaning for dirt, boiled in 1 : 2 chromic acid solutions for sometime for alkali/acid removal, and rinsed in distilled water. Subsequently, the slides were dipped in acetone, subjected to an ultrasonic cleaning to ensure a dirt and dust free slide, and dried by an electric air blower. Finally, the slides were wiped with lint free tissue paper and transferred to a dust free chamber.

First, pellets of 10 mm diameter were made from MgO powder obtained by burning of magnesium ribbon in air and sol–gel technique using a cold press at 4 ton and then sintered at 1000°C for 14 h. Magnesium acetate tetrahydrate $[(CH_3COO)_2Mg{\cdot}4H_2O]$ from E. Merck (India) Ltd., ethyl alcohol (C_2H_5OH) from Hayman Ltd., Essex and oxalic acid $[(COOH)_2{\cdot}2H_2O]$ from Ranbaxy Laboratories Ltd. are used as the raw materials for synthesis of sol–gel MgO and magnesium ribbon from Loba Chemical Ltd., India was used for combustion method. Chemical specifications of the raw materials are given in table 1.

A HHV vacuum coating unit model 12A4D-SC equipped with a 6 kV electron beam gun was employed to make magnesium oxide films at a pressure of $\sim 10^{-5}$ torr. The emission current in the range 60–80 mA was found to be suitable for the evaporation of magnesium oxide from the pellet put in a copper hearth. The deposition time was kept constant for all the films. The deposition rate is dependent on the electron beam voltage and emission current, which was again, kept constant for all the films. Thin films were prepared by maintaining substrates at a fixed distance and varying the time (up to 15 min maximum) of deposition. The thin films were then taken out of the bell jar and stored in a vacuum desiccator. Annealing of thin films was done at 500°C in air or oxygen ambient as per details given in table 2 with respective sample codes.

Various techniques employed for characterization of MgO thin films included scanning electron microscopy (SEM), atomic force microscopy (AFM) and ultraviolet visible spectroscopy. Thickness of MgO thin films was determined by Alpha-Step 500 Profiler. For observing the microscopic nature of the thin films, a scanning electron microscope (SEM) model FEI Quanta 200 was used in the secondary electron mode. Surface roughness of thin films was examined in an atomic force microscope of Molecular Imaging, USA, in acoustic a.c. mode at a scan rate 1·5–2·2 lines/s in air at room temperature. Its cantilever was NSC 12 (C) from MikroMasch with force constant of 4·5 N/m at a frequency of 160 KHz. Optical percentage transmittance (T) and absorbance (A) of magnesium oxide thin films were measured in the wavelength range 200–800 nm with a UV/vis spectrometer, Perkin Elmer, model Lambda 40.

3. Results and discussion

Figure 1 shows the morphology of thin films prepared by e-beam evaporation of MgO powder synthesized by combustion of magnesium ribbon (group C) and sol–gel process (group F) as observed in SEM in SE mode. While the films of group C are quite thick (2927 Å) displaying large line roughness and cross linking morphology (figures 1 (a)–(d)), those with group F (429 Å) are thin, very smooth

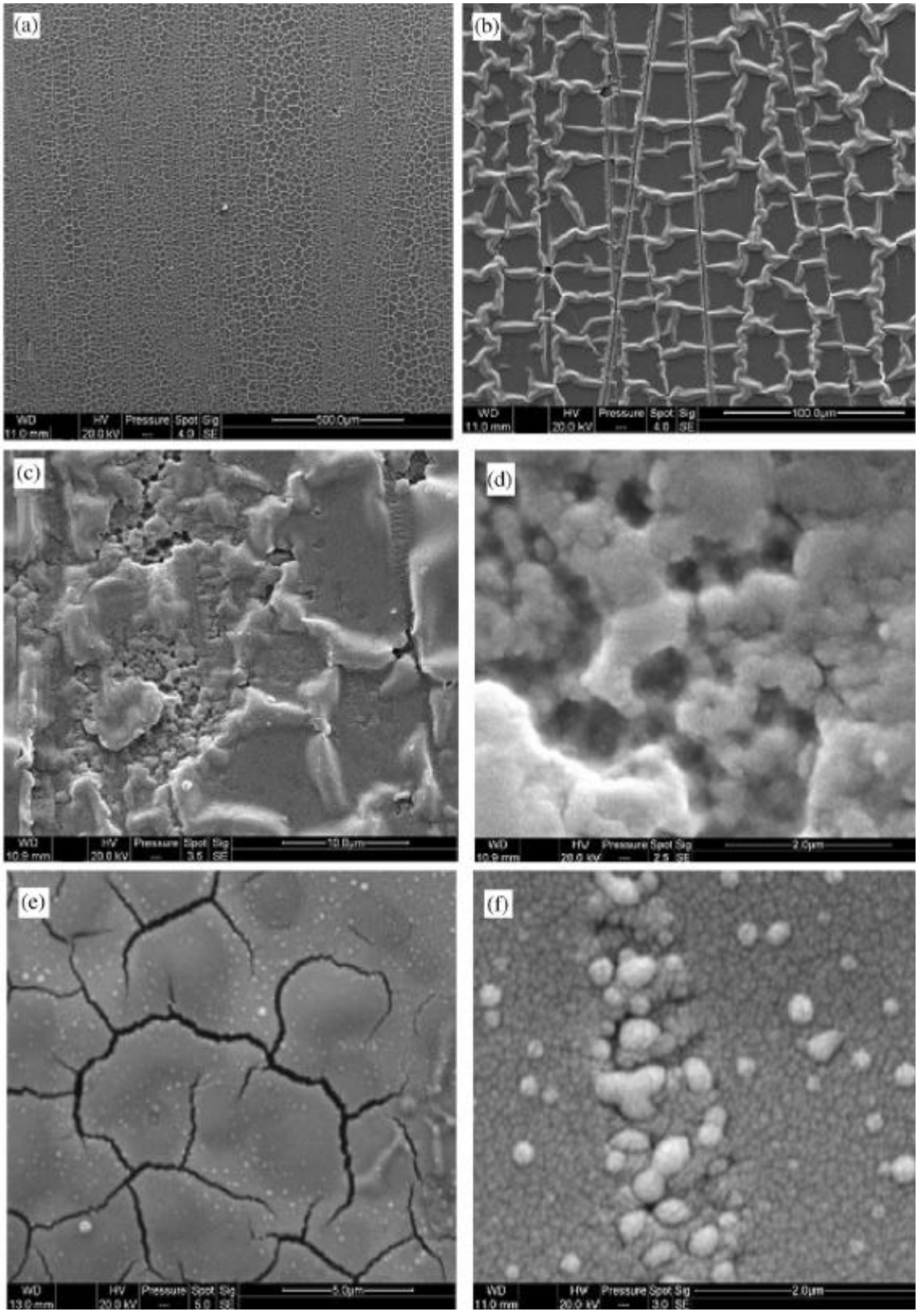

Figure 1. Scanning electron micrographs of MgO thin films prepared by e-beam evaporation from powder synthesized (**a**)–(**d**) by combustion of magnesium ribbon as prepared [group C] and (**e**)–(**f**) by sol–gel process as prepared [group F].

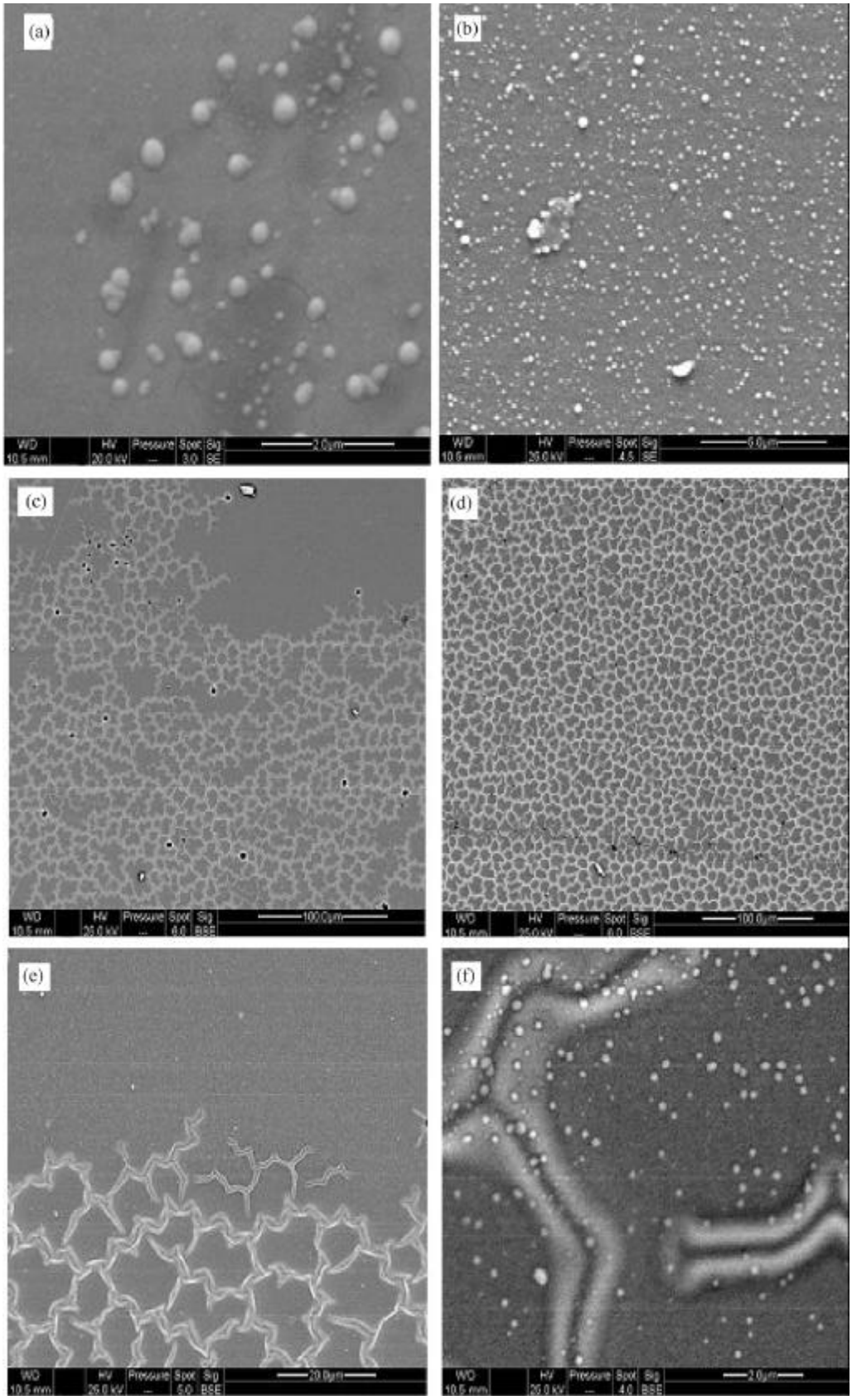

Figure 2. Scanning electron micrographs of MgO thin films prepared by e-beam evaporation from powder synthesized (**b**)–(**f**) by sol–gel process after annealing at 550°C in oxygen [group D] and (**a**) by combustion of magnesium ribbon after annealing at 550°C in air [group B].

with grain-like structure and zigzag discontinuities/cracks at places (like boundaries) (figures 1(e), (f)). The films produced with MgO powder obtained by sol–gel process on annealing at 500°C in oxygen (group D), became nearly continuous and show distribution of spherical shape particles (figure 2(b)). After annealing in air at 500°C, e-beam evaporated thin films of MgO powder synthesized by combustion of magnesium ribbon (group B) exhibit morphology as shown in figure 2(a). SEM observation indicates presence of thick and prominent chain-like boundary regions all over as in group C thin films obtained by MgO powder synthesized by combustion of magnesium ribbon without annealing (figures 1(a), (b)).

At other places, microstructure has chain-like regions but not necessarily distributed, e.g. (figures 2(c)–(f)). This suggests that boundary-like regions may possibly arise due to formation of a different compound, such as magnesium hydroxide [$Mg(OH)_2$] as MgO has a tendency to absorb water very quickly. In a polycrystalline material, grain boundaries are considered as the disordered regions and hence more reactive. It is believed that the formation of magnesium hydroxide occurs in such regions and grows further to cover up the whole film like a zigzag mesh (depicting a self assembled pattern) (figure 1(b)). Boundary-like regions being thick show the mesh structure prominently and has large line roughness as well whereas the mesh in group D film is much finer (figure 2(d)). The details of MgO films not depicting chain-like structure with poor contrast in SEM are observed under AFM. The atomic rearrangement processes in thin films are mainly guided by four basic phenomena: (a) shadowing, (b) surface diffusion, (c) bulk diffusion and (d) desorption (Milton 2001). The last three are quite common, while shadowing actually occurs in special situations and de-

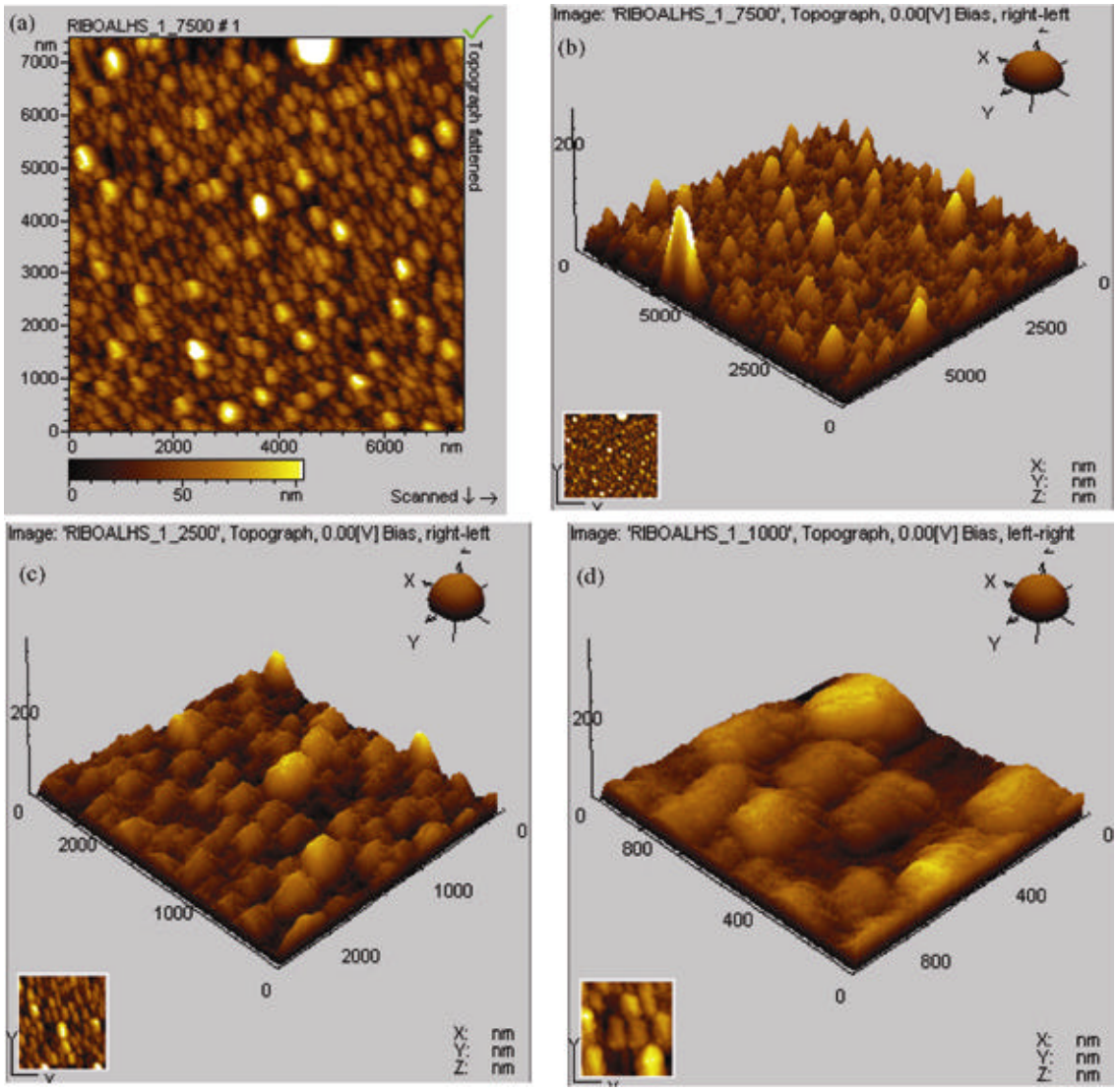

Figure 3. AFM images of e-beam evaporated MgO thin films synthesized by pellet of MgO powders obtained by burning magnesium ribbon and annealed at 500°C in oxygen (group A).

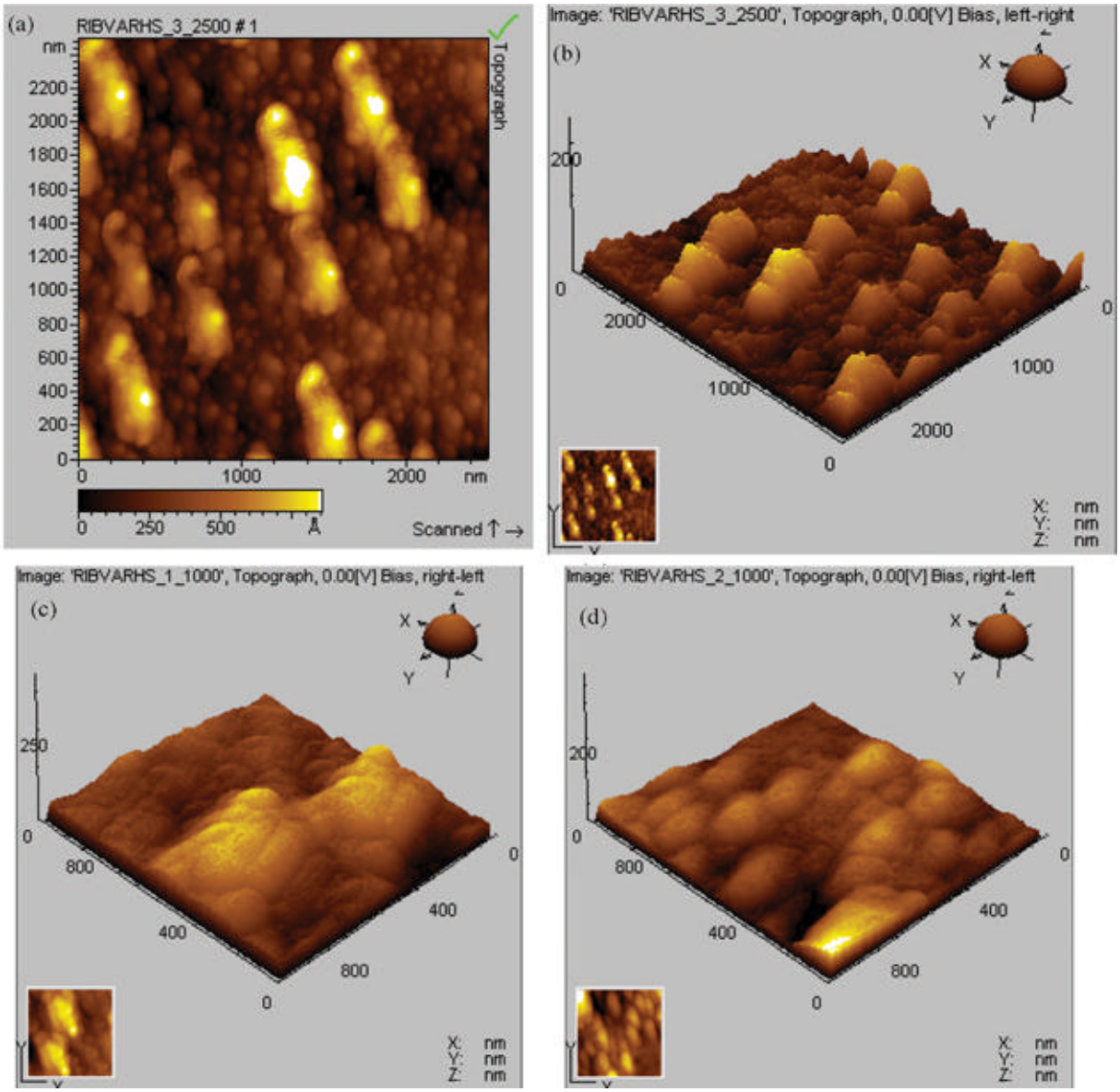

Figure 4. AFM images of e-beam evaporated MgO thin films synthesized by pellet of MgO powders obtained by burning magnesium ribbon and annealed at 500°C in air (group B). The images are taken at three different regions (**a**/**b**, **c**, **d**).

pends on the geometric constraint imposed by the roughness of the growing film and the line of sight impingement of the arriving atoms. In this work, AFM observation studies have been made of the e-beam evaporated thin films synthesized by MgO powder obtained by burning magnesium ribbon and sol–gel process to understand the nature of film growth.

Figure 3 shows AFM images of group A thin film synthesized by MgO powders obtained by combustion of magnesium ribbon after annealing at 500°C in oxygen. These clearly show (figures 3(b)–(c)) faceted columnar microstructure of varied height resulting perhaps due to anisotropy of the sticking coefficient and mobility of adatoms. Shadowing is very prominent here and columns are elongated along a preferential growth direction. Some small regions are relatively flat as well (figure 3(d)). Figure 4 shows AFM images of MgO thin films synthesized by MgO powders obtained by burning magnesium ribbon after annealing at 500°C in air (group B). In figure 4(b) coarsening and agglomeration of grains with some truncated cone-like columnar growth are seen. These dome-shaped grains have same size (average size, 260–370 nm and thickness, 82 nm) with faintly defined boundaries. A preferential growth in a particular direction has still been

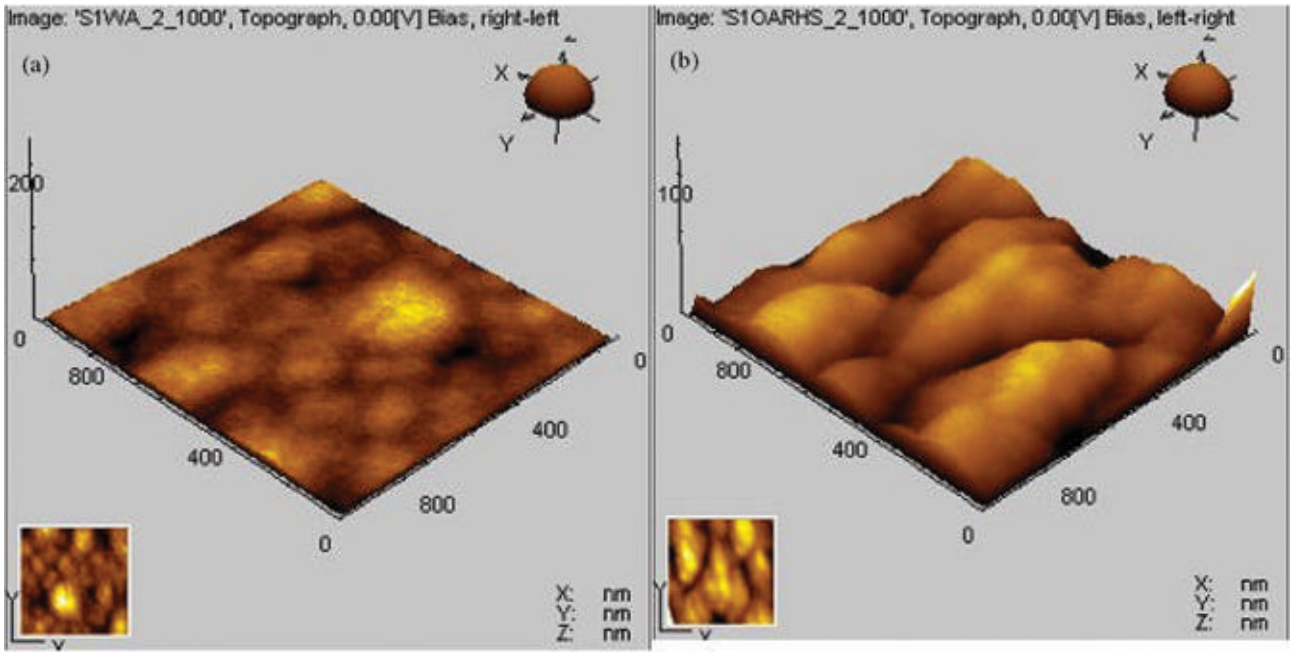

Figure 5. AFM images of e-beam evaporated MgO thin films synthesized by MgO pellet obtained by sol–gel method (**a**) as prepared (group F) and (**b**) after annealing at 500°C in oxygen (group D).

Table 3. RMS roughness values obtained through AFM experiment in different scan areas (Å).

Sample code	MgO powder synthesis route	Processing and treatment	Scan area (nm^2)	*RMS roughness (Å)
A	Combustion of magnesium ribbon	Annealed at 500°C in presence of oxygen with a flow rate of 30 cc/s	1000 × 1000	145·9
			2500 × 2500	149
			7500 × 7500	254
B (region 1)	Combustion of magnesium ribbon	Annealed at 500°C in presence of air	1000 × 1000	173·9
(region 2)			1000 × 1000	112·9
(region 3)			2500 × 2500	172
D	Sol–gel process	Annealed at 500°C in presence of oxygen with a flow rate of 30 cc/s	1000 × 1000	69·4
			2500 × 2500	77·7
E	Sol–gel process	Annealed at 500°C in presence of air	2500 × 2500	71
F	Sol–gel process	Films as prepared (without annealed)	1000 × 1000	17·4

observed. Figures 4(c), (d) show island type plateau regions. The next group of AFM images (figures 5, 6) show films prepared with sol–gel derived MgO powder as such and after annealing at 500°C in oxygen (group D) and in air (group E). No preferential growth is seen in figure 6(a), but figure 5(b) shows bulging of grains assuming nearly the same height with smooth rounded surface. Figure 6(b) also shows pronounced growth of elongated shape particles with non-uniform sizes, corrugated surface and rms roughness of ~ 69·4 Å. Figure 6(d) represents the annealing behaviour in air. Hence there is isolated growth of dome-shaped particles. The rms roughness values of various MgO films obtained from AFM observations are given in table 1.

It may be noted that group F films show less roughness values than the values reported earlier for MgO (Menon and Bullard 1999; Kim *et al* 2000, 2004; Jung *et al* 2002), whereas the other films (groups D and E) correspond to a reasonably good degree of smoothness (roughness, < 80 Å).

So, it can be inferred that the oxygen annealed films are more transparent than air annealed ones due to less roughness and hence more uniformity. A comparison between films prepared by sol–gel process and by combust-

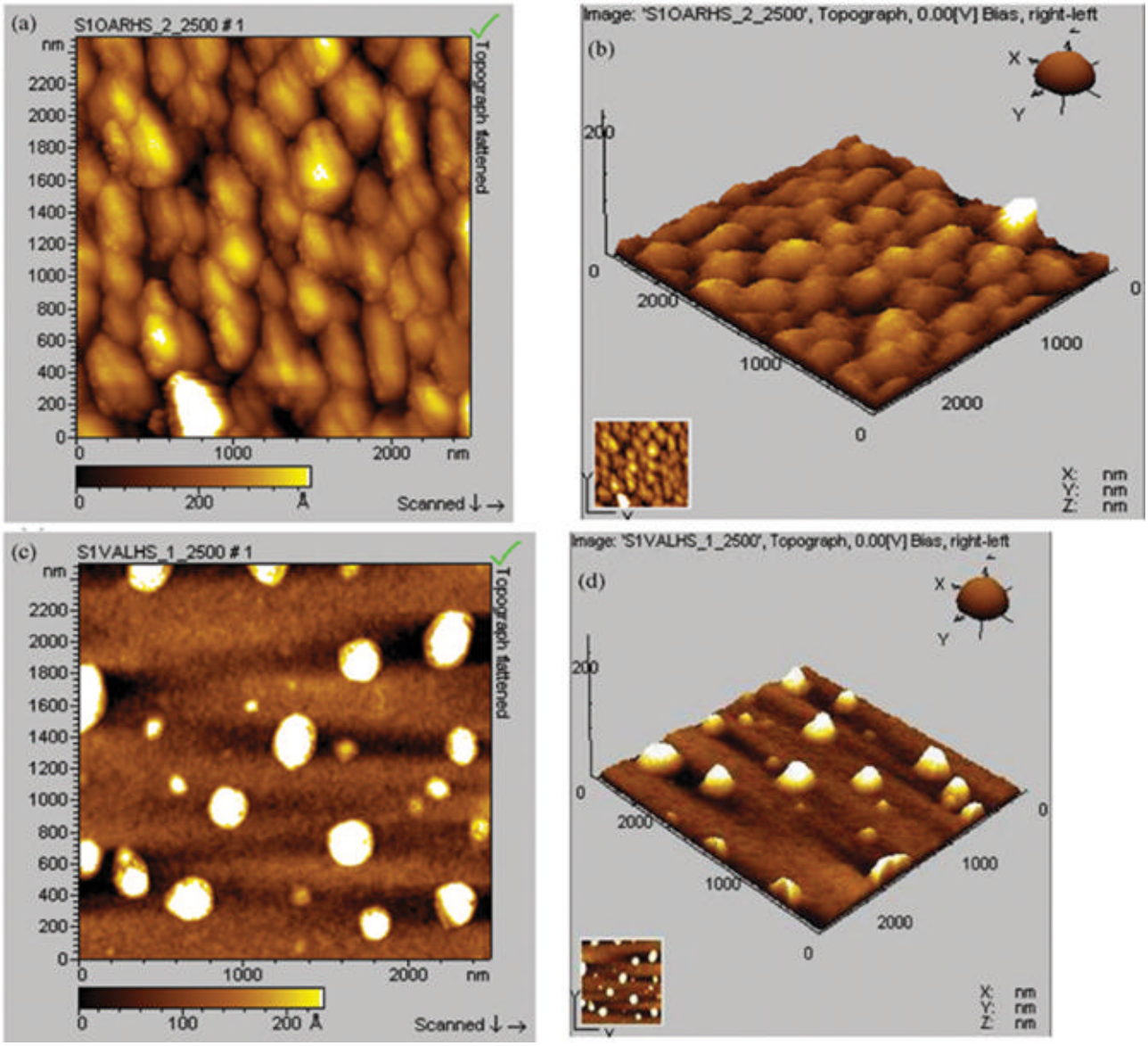

Figure 6. AFM images of e-beam evaporated MgO thin films synthesized by MgO pellet obtained by sol–gel method after annealing at 500°C (**a**, **b**) in oxygen (group D) and (**c**, **d**) in air (group E).

ion of ribbon shows the former one to be more transparent. This inference is consistent with UV spectroscopy transmittance data described possibly due to finer grain size. In conclusion, the film growth mode appears to be of 3D Stranski–Krastanov type (layer plus island growth) for MgO.

The RMS roughness values given here in table 3 are reported after subtracting the roughness values for glass substrate, which is found as 7·1 Å and 11 Å, respectively for an area of 1000×1000 and 2500×2500 nm^2, respectively.

The transmission (%) vs wavelength plots of different thin film samples deposited on glass substrates are shown in figure 7. The nature in the plots is the same with transmission at nearly 90% for all except group C sample (where % $T \sim 78$) in the wavelength range 350–800 nm. The results clearly demonstrate that annealing improves the transparency for thin films produced with MgO powder obtained by combustion of magnesium ribbon. Also sol–gel derived MgO powder thin film invariably shows high transmission due to the annealing process. There is a dip invariably present at slightly after 350 nm, the transmission decreases sharply indicating strong absorption of the radiation.

4. Conclusions

The SEM images discover a very unique self-assembled kind of a structure which has been assigned to the formation of $Mg(OH)_2$, however, the propagation route of the network

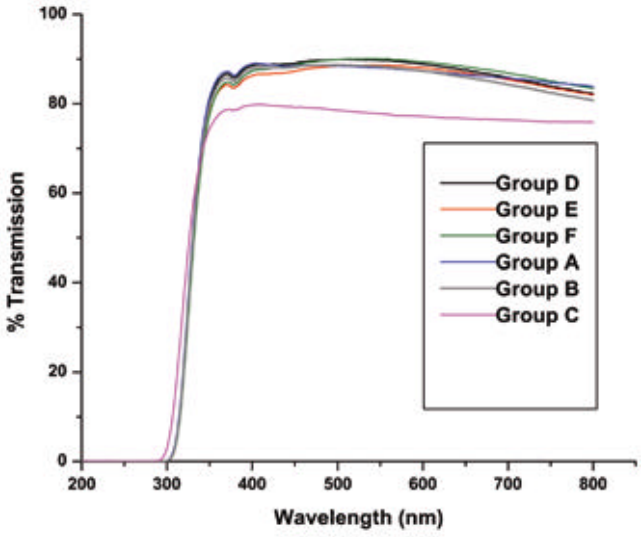

Figure 7. Transmission vs wavelength plots of e-beam evaporated MgO thin films. MgO thin films prepared by MgO powder/pellet from combustion of magnesium ribbon without annealed (group C), air annealed (group B) and annealed in oxygen (group A) and sol–gel process without annealed (group F), air annealed (group E) and annealed in oxygen (group D).

cannot be specified at this stage. This study shows that hydration does not depend on the post treatments on the film e.g. annealing as both groups C and D films are affected by this. The structures of the mesh formed are also different in these two films.

AFM studies have been carried out and after comparison of the microstructure of different films, it can be said that, the results obtained here are quite different from what have been observed in case of structure-zone model for evaporated films (mostly done for metals). The growth of the films is only observed after annealing with oxygen annealing providing support for pronounced columnar growth. The columns of different shapes have also been observed. Air annealing is shown to produce truncated columns. However, a much in-depth analysis is needed to have a final say on this issue.

Acknowledgements

The authors are grateful to Mr Mohit Lakhera, Vac. Tech. Engineers, for his help and support in the preparation of thin films. We also extend our sincere thanks to Mr Dinesh Deva in doing the AFM experiment.

References

Boeuf J P 2003 *J. Phys. D Appl. Phys*. **36** R53

Boo J H, Yu K S, Koh W and Kim Y 1996 *Mater. Lett*. **26** 233

Chakrabarti S, Ganguli D, Chaudhuri S and Pal A K 2002 *Mater. Lett*. **54** 120

Chakrabarti S, Ganguli D and Chaudhuri S 2003 *Mater. Lett*. **57** 4483

Chowdhury A 2005 *Synthesis and characterization of magnesium oxide powder and electron beam evaporated thin films*, M.Tech. Thesis, IIT Kanpur

Ho I C, Xu Y and Mackenzie J D 1997 *J. Sol-Gel Sci. Technol*. **9** 295

Huang Ron and Kitai Adrian H 1992 *Appl. Phys. Lett*. **61** 1450

Imai F *et al* 1992 *Appl. Surf. Sci*. **60–61** 770

Jung Hyun Suk, Lee Jung-Kun, Hong Kug Sun and Youn Hyuk-Joon 2002 *J. Appl. Phys*. **92** 2855

Kim B I, Hung J W, Jeung G T, Moon S H, Lee D H, Shin T U and Khim Z G 1994 *J. Vac. Sci. Technol*. **B12** 1631

Kim Jong-Kuk, Lee Eun-Sung, Kim Dong-Ho and Kim Do-Geun 2004 *Thin Solid Films* **447–448** 95

Kim R, Kim Y, Cho J and Park J W 2000 *J. Vac. Sci. Technol*. **A18** 2493

Menon M and Bullard J W 1999 *Mater. Chem*. **9** 949

Milton Ohring 2001 *The materials science of thin films* (New York: Academic Press) Ch. 9

Nashimoto K, Fork D K and Geballa T H 1992 *Appl. Phys. Lett*. **60** 1199

Park Chung-Hoo, Kim Young-Kee, Lee Sung-Hyun, Lee Woo-Geun and Sung Youl-Moon 2000 *Thin Solid Films* **366** 88

Phillipsa Julia M 1996 *J. Appl. Phys*. **79** 1829